Acta Crystallographica Section C
Crystal Structure Communications
ISSN 0108-2701

New vanadium(IV) and titanium(IV) oxyfluorotellurates(IV): $V_2Te_2O_7F_2$ and $TiTeO_3F_2$

Jean Paul Laval* and Nefla Jennene Boukharrata

Science des Procédés Céramiques et de Traitements de Surface, UMR–CNRS 6638, Faculté des Sciences et Techniques, Université de Limoges, 123 Avenue A. Thomas, Limoges 87060, France
Correspondence e-mail: jean-paul.laval@unilim.fr

Received 29 October 2008
Accepted 7 November 2008
Online 13 December 2008

As part of a continuing study of oxyfluorotellurates(IV), materials likely to present interesting nonlinear optical properties, two new phases, titanium(IV) tellurium(IV) trioxide difluoride, $TiTeO_3F_2$, and divanadium(IV) ditellurium(IV) heptaoxide difluoride, $V_2Te_2O_7F_2$, have been characterized and present, respectively, titanium and vanadium in the tetravalent state. The $TiTeO_3F_2$ structure is based on linear double rows of TiO_3F_3 polyhedra sharing vertices. These rows are connected to adjacent rows *via* two vertices of Te_2O_5 bipolyhedra. The Te, Ti, one F and two O atoms are on general positions, with one O and F statistically occupying the same site with half-occupancy for each anion. One O and one F occupy sites with *.m.* symmetry. The $V_2Te_2O_7F_2$ structure consists of zigzag chains of VO_4F_2 octahedra alternately sharing O—O and F—F edges. These chains are connected *via* Te_2O_5 bipolyhedra, forming independent mixed layers. The Te, V, one F and three O atoms are on general positions while one O atom occupies a site of $\overline{1}$ symmetry. In both phases, the electronic lone pair *E* of the Te^{IV} atom is stereochemically active. A full O/F anionic ordering is observed in $V_2Te_2O_7F_2$, but in $TiTeO_3F_2$ one of the six anionic sites is occupied by half oxygen and half fluorine, all the others being strictly ordered. These compounds represent new members of a growing family of oxyfluorotellurates(IV), including the recently characterized members of formula $MTeO_3F$, *M* being a trivalent cation. As was true for the previous members, they are characterized by an unusually high thermal and chemical stability in relation to the absence of direct Te—F bonds.

Comment

In $TiTeO_3F_2$, the $Ti1^{4+}$ cation is coordinated by two O atoms (O1 and $O2^{iv}$), two F atoms (F2 and F3) and two mixed-anion sites O4/F1 and $(O4/F1)^{iv}$ (half occupied by O and half by F anions) [symmetry code: (iv) $x+\frac{1}{2}, y, -z+\frac{3}{2}$]. The TiO_3F_3 octahedra (Fig. 1) are slightly distorted in that the Ti1—F3 bond is significantly shorter than the others (Table 1). These octahedra share F2 and O4/F1 vertices, forming infinite double rows of ReO_3-type (Hyde & Andersson, 1989) extending along [100].

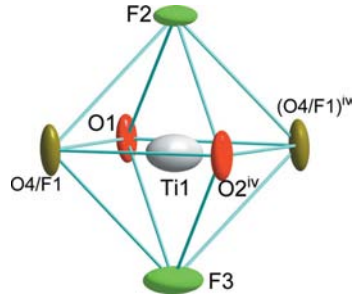

Figure 1
The coordination polyhedron of Ti1 in $TiTeO_3F_2$. [Symmetry code: (iv) $x+\frac{1}{2}, y, -z+\frac{3}{2}$.]

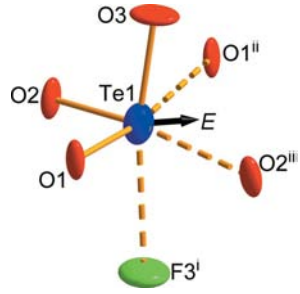

Figure 2
The Te coordination in $TiTeO_3F_2$. The arrow indicates the direction towards which the lone pair *E* points. [Symmetry codes: (i) $-x+1, -y, -z+1$; (ii) $x-\frac{1}{2}, y, -z+\frac{1}{2}$; (iii) $x+\frac{1}{2}, y, -z+\frac{1}{2}$.]

The $Te1^{4+}$ atom is surrounded by three strongly bonded O atoms, *viz.* O1, O2 and O3, forming a tetrahedron whose fourth corner corresponds to the direction of the stereochemically active lone pair *E* (Fig. 2). Two TeO_3 polyhedra share an O3 vertex, forming a slightly angulated $[Te_2O_5]$

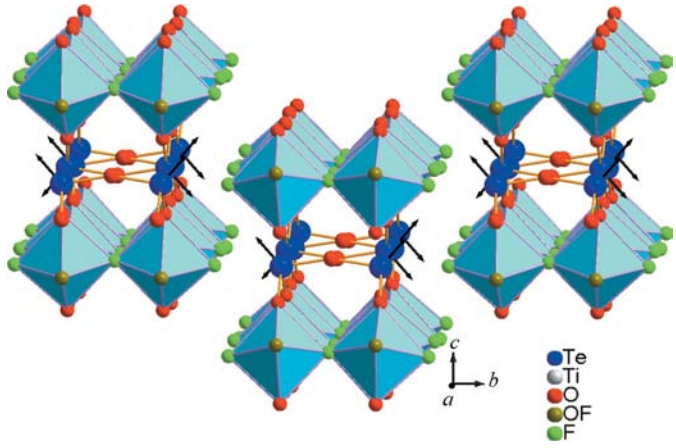

Figure 3
A perspective view showing the double rows of titanium octahedra and their connections to the Te_2O_5 units.

 doi:10.1107/S0108270108036755

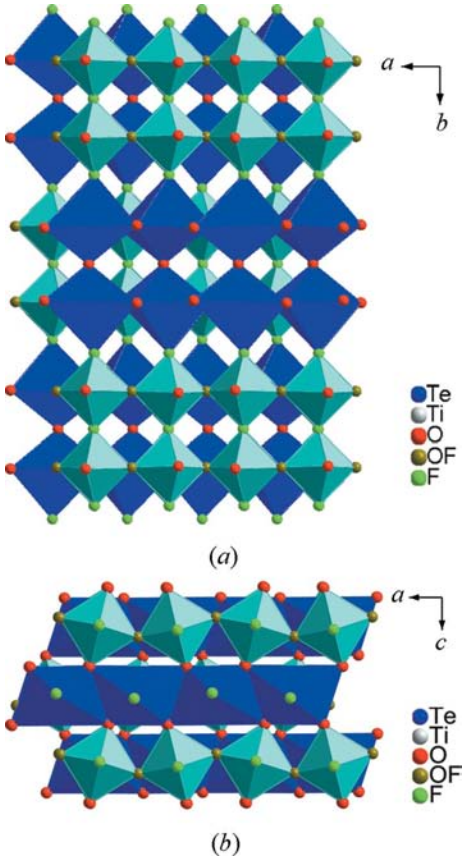

Figure 4
Projections on to (*a*) the *ab* plane and (*b*) the *ac* plane, showing the smooth three-dimensional framework in $TiTeO_3F_2$.

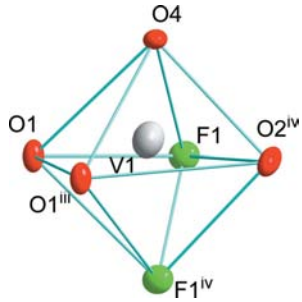

Figure 5
The coordination polyhedron of V1 in $V_2Te_2O_7F_2$. [Symmetry codes: (iii) $-x, -y+1, -z+1$; (iv) $-x+1, -y+1, -z+1$.]

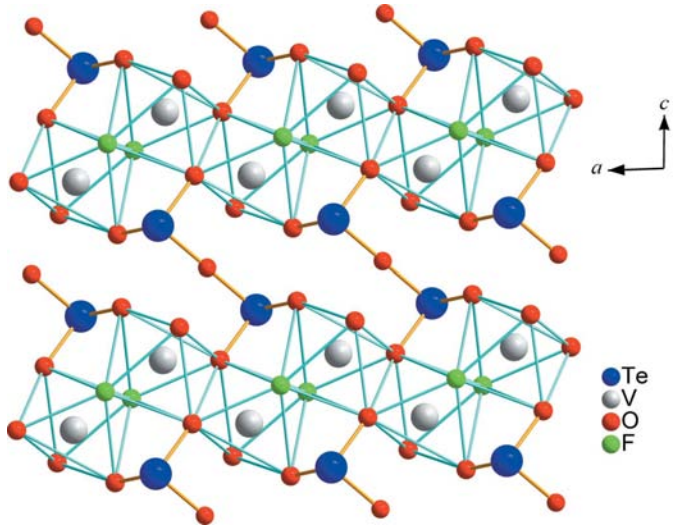

Figure 6
A projection of $V_2Te_2O_7F_2$ on to the *ac* plane, showing the V chains connected *via* Te_2O_5 units.

bipolyhedron with Te1—O3—Te1^{v} = 161.1 (4)° [symmetry code: (v) $x, -y+\frac{1}{2}, z$] (Fig. 3).

Along [001], successive double rows of slightly tilted TiO_3F_3 octahedra are connected *via* O1 and O2 vertices to these $[Te_2O_5]$ bipolyhedra (Fig. 3), together forming double sheets in which Te and Ti cations form a rather regular cubic close-packed framework with Ti1—Ti1, Ti1—Te1 and Te1—Te1 distances ranging from 3.622 (2) to 3.908 (1) Å. The lone pairs of $Te1^{4+}$ are directed towards the free space between the double sheets. Successive double sheets along [010] are shifted by $c/2 + a/2$.

The Te atom is also weakly bonded to three other anions, *viz*. F3^{i}, O1^{ii} and O2^{iii} [symmetry codes: (i) $-x+1, -y, -z+1$; (ii) $x-\frac{1}{2}, y, -z+\frac{1}{2}$; (iii) $x+\frac{1}{2}, y, -z+\frac{1}{2}$], giving a distorted TeO_5F octahedron, the lone pair *E* pushing away the triangular face formed by these latter three anions (Fig. 2). These TeO_5F distorted octahedra, associated in bioctahedra by sharing O3 vertices, also form double rows extending along [100] by sharing O1—O2 edges.

The packing of double rows of TiO_3F_3 and TeO_5F octahedra alternating along the [010] and [001] directions by sharing, respectively, F3 and O1 or O2 vertices allows a smooth three-dimensional framework to be defined (Fig. 4*a* and *b*), with (010) grossly hexagonal plane nets (c/a = 0.878, instead of 0.866 for a perfect hexagonal net described in orthorhombic symmetry). These plane nets are composed of the association of parallel rows of corner-sharing TiO_3F_3 tilted octahedra and edge-sharing TeO_5F distorted octahedra (Fig. 4*a*), all these octahedra sharing all their apices along [010] (Fig. 4*b*).

The bond-valence calculations (Brown, 1981) reported in Table 2 show without any ambiguity that the Ti cations are in the tetravalent state. This is in agreement with the colourless crystals obtained after thermal treatment (see *Experimental*). In spite of the use of a glove-box under dried argon, Ti^{3+} was completely oxidized to Ti^{4+} during the synthesis process. As TiF_3 itself is generally stable in such conditions, it seems that, in the presence of tellurium(IV) oxide, Ti^{3+} tends to oxidize to Ti^{4+}.

In $V_2Te_2O_7F_2$, the $V1^{4+}$ cation is coordinated by four O and two F atoms. The distorted VO_4F_2 octahedra (Fig. 5 and Table 3) form 'zigzag' twisted chains parallel to the [100] direction by alternately sharing O1—O1 and F1—F1 edges with rather long V1—O1 and V1—F1 bonds (Fig. 6). In these chains, the O4 anion is only connected to one V atom, by a very short bond. Such behaviour is not unexpected for a 'terminal' anion in the presence of edge-sharing, and this

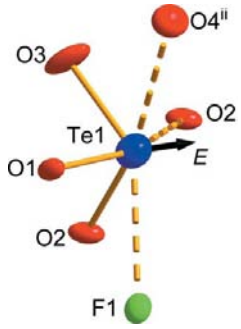

Figure 7
The Te coordination in $V_2Te_2O_7F_2$. The arrow indicates the direction towards which the lone pair *E* points. [Symmetry codes: (i) $-x+1, -y+1, -z$; (ii) $-x, -y+2, -z+1$.]

strong bond results from the displacement of V cations in the chain, the V1···V1 distance being 3.321 (1) Å for a V1–(F1—F1)–V1 bridge and only 3.089 (1) Å for a V1–(O1—O1)–V1 bridge. The V cation is not centred in the VO_4F_2 octahedron, but rather shifted along the O4—F1^{iv} [symmetry code: (iv) $-x+1, -y+1, -z+1$] axial direction, as readily observed in Fig. 5, and its coordination should be considered as 5+1 instead of 6. The opposite V1—F1^{iv} bond is logically the longer one.

Several V^{IV} oxyfluorides are known. In most, V^{IV} is located in a more or less distorted octahedron. For example, in $BaVOF_4$ (Crosnier-Lopez, Duroy & Fourquet, 1994), the VOF_5 octahedron has similar features to VO_4F_2 in the present phase, namely a very short V—O distance of 1.621 (4) Å, four medium-size V—F distances extending from 1.917 (3) to 1.985 (4) Å and a longer V—F bond, opposite the shorter one, of 2.193 (3) Å. Therefore, V^{IV} is shifted from the centre of the octahedron, as in $V_2Te_2O_7F_2$. Similar behaviour occurs in $CsVOF_3$ [Aldous *et al.*, 2007; short bond = 1.600 (7) Å] and also in some V^{V} oxyfluorides such as $NaVO_2F_2$ (Crosnier-Lopez, Duroy, Fourquet & Abrabri, 1994). This behaviour results from the formation of terminal 'vanadyl' V═O groups, as described in a comparative study of some 'spin-ladder'-like $MVOF_3$ alkaline vanadium oxyfluorides (Aldous *et al.*, 2007) in which V—V interactions are in the range 3.31–3.34 Å for V–(F—F)–V edge-bridging, quite similar to our result. However, there is no equivalent to the very short V1···V1 interaction (3.089 Å), observed in $V_2Te_2O_7F_2$ and resulting from the V1–(O1—O1)–V1 bridge, in the close 'spin-ladder' $(VO)_2P_2O_7$ phase. In this last structure, the V—V distance is around 3.2–3.3 Å. Interesting magnetic properties should be expected for $V_2Te_2O_7F_2$.

The $Te1^{4+}$ anionic environment is almost the same as in $TiTeO_3F_2$ (Table 3 and Fig. 7). Each Te atom shares two O atoms (O1 and O2) with two adjacent V atoms of the same chain. The third O atom, O3, is connected to a second Te atom, so forming a strong $[Te_2O_5]$ unit, itself connected to the adjacent chain by sharing O1 and O2 anions with two V atoms of this chain (Fig. 6). The connection of the V chains through linear $[Te_2O_5]$ units (Te1—O3—Te1^{v} = 180°) [symmetry code: (v) $-x, 1-y, -z$] forms independent layers, stacked along

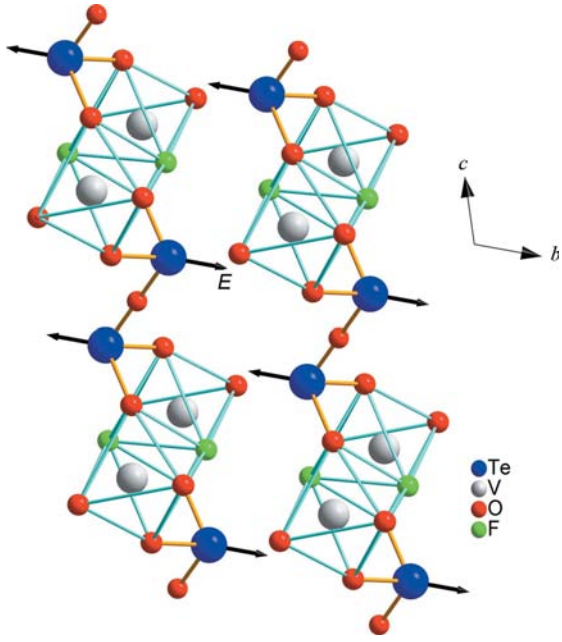

Figure 8
A projection of $V_2Te_2O_7F_2$ on to the *bc* plane, showing the mixed layers and the lone pairs *E* directed towards the intersheet regions.

[010], with the electronic lone pairs *E* of $Te1^{4+}$ directed towards the intersheet space (Fig. 8).

Bridging $[Te_2O_5]$ units are also described in $M_2Te_4O_{11}$ (*M* = Lu, Y, La–Nd and Sm–Yb) (Höss *et al.*, 2005; Castro *et al.*, 1990; Weber *et al.*, 2001; Ijjaali *et al.*, 2003; Meier & Schleid, 2004; Shen & Mao, 2004). However, in $Lu_2Te_4O_{11}$, for example, the Te—O—Te bridge angle (138.9°) is significantly smaller than in either $TiTeO_3F_2$ or $V_2Te_2O_7F_2$, and the $[Te_2O_5]$ units connect layers of edge-sharing LuO_8 polyhedra instead of chains of edge-sharing VO_4F_2 octahedra. The extensive angle range possible inside the $[Te_2O_5]$ bipolyhedron is likely to be a good means of adaptation to interconnect various types of polyhedra layers in different oxyfluorotellurates.

In $V_2Te_2O_7F_2$, the Te atom is also weakly bonded to three other anions, *viz.* F1, O4^{ii} and O2^{i} [symmetry codes: (i) $-x+1, -y+1, -z$; (ii) $-x, -y+2, -z+1$], giving a very distorted TeO_5F octahedron, the lone pair *E* pushing away the triangular face formed by these latter three anions (Fig. 7). These TeO_5F distorted octahedra also form zigzag chains parallel to the [100] direction by sharing alternately an O2—O2 edge and an O3 corner. These chains are inserted between and connected to the VO_4F_2 octahedra through O2—F1 and O1—F1 edges, so forming twisted layers (Fig. 9). These layers are weakly connected along [010] *via* O4 vertices, giving a smooth three-dimensional framework.

The bond valences calculated for all cationic and anionic sites (Brown, 1981) are reported in Table 4. If only the three strong Te1—O interactions are considered, the calculated bond valence is 3.87 ē. If the three weaker interactions are added, the calculated bond valence for the Te site is 4.34 ē, which confirms the presence of $Te1^{4+}$. The V site, originally supposed to be occupied by V^{3+} because vanadium trifluoride

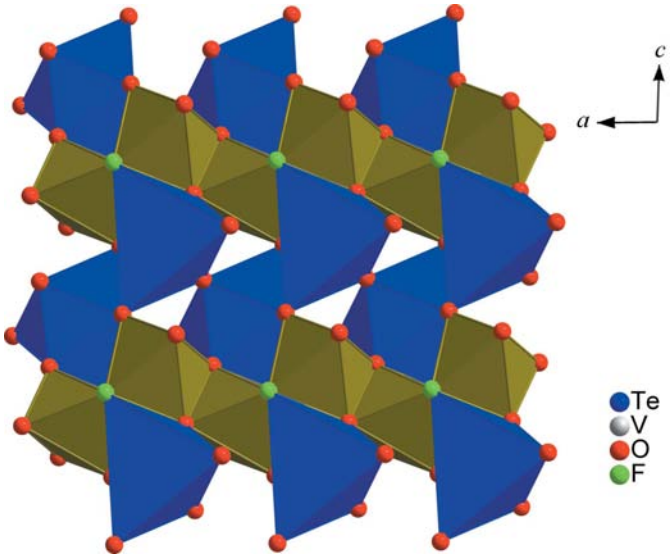

Figure 9
A projection of $V_2Te_2O_7F_2$ on to the *ac* plane, showing the alternation and connection of 'zigzag' chains of Te and V polyhedra.

was used in the synthesis process, has been implicitly considered above as a V^{4+} cation after examination of the V anionic octahedron, much closer to those described with V^{4+} or even V^{5+} than to the trivalent state. The calculation of bond valences shows a valence ν = 3.71 ē in presupposing V^{3+} and ν = 3.89 ē with V^{4+} cations, using Ro and B values tabulated by Brown. The same calculation applied to O and F anions shows that the sites labelled O1, O2 and O3 are undoubtedly occupied by O, with ν being 2.33, 2.10 and 2.72, respectively, with V supposed tetravalent, the site F1 being occupied by F (ν = 0.86). The O4 site is more difficult to define because its valence is 1.31 if it is occupied by F and 1.56 by O. It is therefore likely, as suggested by the structural features of the vanadium octahedron and by the bond-valence calculations, that, in the present phase, all or the greater part of vanadium cations are oxidized during the synthesis process from trivalent to tetravalent. The chemical formula, which should have been $V_2Te_2O_5F_4$ for trivalent vanadium, is more likely $V_2Te_2O_7F_2$ with tetravalent vanadium. However, a higher oxidation in V^{5+}, giving a pure oxide $V_2Te_2O_9$, disagrees with the bond-valence calculation and must be ruled out.

In conclusion, $TiTeO_3F_2$ and $V_2Te_2O_7F_2$, although belonging to rather different structure types, present some analogous features. They are derived from regular octahedral structures by assimilating distorted octahedral Te^{4+} environments. As in the oxyfluorotellurates of trivalent metals $MTeO_3F$ [M = (Fe, Cr, Ga) (Laval *et al.*, 2008), Sc, In (Jennene Boukharrata *et al.*, 2008)] described previously, no short Te—F bonds are present, which greatly increases the thermal and chemical stability of these phases. All F anions are directly linked to trivalent or tetravalent metals, giving various kinds of octahedra (TiO_3F_3, VO_4F_2, ScO_4F_2, InO_5F and FeO_4F_2) connected *via* O or F vertices or edges, so forming various structural units.

Therefore, the oxyfluorotellurates of trivalent and tetravalent metals constitute a family which, by its original structures and their stability, increases the field of phases potentially available for optical or magnetic applications.

Experimental

$TiTeO_3F_2$ was prepared by solid-state reaction of TiF_3 (Aldrich, 99%) and TeO_2, which was prepared in the laboratory by decomposition at 823 K of commercial H_6TeO_6 (Aldrich, 99.9%) under flowing oxygen. Owing to the hygroscopic character of TiF_3, sample preparation was carried out in a glove-box under dried argon. An intimate mixture of TiF_3 and TeO_2 in a 1:1 molar ratio was placed in a sealed platinum tube. Colourless prismatic single crystals, air stable and suitable for X-ray diffraction study, were prepared by increasing the temperature to 773 K at a rate of 5 K min^{-1}, keeping it stable for 48 h, and then slowly cooling the sample (0.1 K min^{-1}) to 673 K and quenching it in cold water. Because of the absence of coloration in the crystals, oxidation from Ti^{3+} to Ti^{4+} was suspected and has been confirmed by the structure determination. Several attempts have shown that this oxidation is systematic, probably resulting from the poor quality and dryness of the commercial product, even though labelled 'pure', and/or oxidation–reduction reactions in the presence of TeO_2.

Single crystals of $V_2Te_2O_7F_2$ were grown in a sealed platinum tube by heating a mixture of VF_3 (Aldrich, 99%) and TeO_2 in a 1.5:1 molar ratio using the same process as for the previous sample, including manipulations in a glove-box. Green–brown rhomboidal single crystals, air stable and suitable for X-ray diffraction study, were obtained.

For both syntheses, the single crystals grow in a more or less molten and out-of-equilibrium multicomponent M–Te–O–F medium likely to contain Te resulting from the redox reaction $4Ti^{3+} + Te^{4+} \rightarrow 4Ti^{4+} + Te^{0}$, but also Te^{IV} oxyfluorides with a very low melting point, as shown in a previous study of the Te^{IV}–O–F phase diagram (Ider *et al.*, 1995). Therefore, the phase composition is only attested by the initial mixture composition and the crystal structure determination.

$TiTeO_3F_2$

Crystal data

$TiTeO_3F_2$
M_r = 261.50
Orthorhombic, *Pnma*
a = 7.3917 (12) Å
b = 16.369 (3) Å
c = 6.4886 (8) Å
V = 785.1 (2) Å^3
Z = 8
Mo $K\alpha$ radiation
μ = 9.40 mm^{-1}
T = 293 (2) K
0.02 × 0.01 × 0.01 mm

Data collection

Bruker–Nonius KappaCCD area-detector diffractometer
Absorption correction: multi-scan (*SADABS*; Bruker 2001)
T_{min} = 0.820, T_{max} = 0.901
20588 measured reflections
1170 independent reflections
970 reflections with $I > 2\sigma(I)$
R_{int} = 0.068

Refinement

$R[F^2 > 2\sigma(F^2)]$ = 0.032
$wR(F^2)$ = 0.078
S = 1.07
1170 reflections
68 parameters
$\Delta\rho_{max}$ = 4.34 e Å^{-3}
$\Delta\rho_{min}$ = −1.77 e Å^{-3}

Table 1
Selected bond lengths (Å) for $TiTeO_3F_2$.

Te1—O2	1.872 (4)	Ti1—F3	1.813 (4)
Te1—O1	1.872 (4)	Ti1—O4/F1^{iv}	1.9057 (10)
Te1—O3	1.8989 (12)	Ti1—O4/F1	1.9084 (10)
Te1—F3^{i}	2.556 (4)	Ti1—O1	1.924 (4)
Te1—O1^{ii}	2.731 (4)	Ti1—O2^{iv}	1.925 (4)
Te1—O2^{iii}	2.764 (4)	Ti1—F2	1.9550 (9)

Symmetry codes: (i) $-x+1, -y, -z+1$; (ii) $x-\frac{1}{2}, y, -z+\frac{1}{2}$; (iii) $x+\frac{1}{2}, y, -z+\frac{1}{2}$; (iv) $x+\frac{1}{2}, y, -z+\frac{3}{2}$.

Table 2
Bond valences in $TiTeO_3F_2$.

	Te1	Ti1	γ_{ij}
O1	1.329/0.130	0.745	2.20
O2	1.330/0.119	0.743	2.19
O3	2×1.235		2.47
O4		0.783/0.777	1.56
F1		0.602/0.597	1.20
F2		0.527	1.05
F3	0.202	0.772	0.97
γ_{ij}	4.35	4.34/4.00	

Table 3
Selected bond lengths (Å) for $V_2Te_2O_7F_2$.

Te1—O3	1.8637 (7)	V1—O4	1.5944 (19)
Te1—O2	1.8710 (18)	V1—F1	1.9480 (15)
Te1—O1	1.9174 (17)	V1—O1	1.9832 (18)
Te1—O2^{i}	2.4888 (19)	V1—O1^{iii}	1.9924 (18)
Te1—F1	2.7385 (17)	V1—O2^{iv}	2.0273 (18)
Te1—O4^{ii}	2.846 (2)	V1—F1^{iv}	2.2156 (17)

Symmetry codes: (i) $-x+1, -y+1, -z$; (ii) $-x, -y+2, -z+1$; (iii) $-x, -y+1, -z+1$; (iv) $-x+1, -y+1, -z+1$.

Table 4
Bond valences in $V_2Te_2O_7F_2$.

	Te1	$V1^{4+}$	γ_{ij}	$V1^{3+}$	γ_{ij}
O1	1.175	0.584/0.569	2.33	0.522/0.510	2.21
O2	1.332/0.251	0.518	2.10	0.464	2.05
O3	2×1.358		2.72		2.72
O4	0.096	1.462	1.56	1.494	1.59
F1	0.123	0.248/0.512	0.86	0.487/0.236	0.85
γ_{ij}	4.34	3.89		3.71	

$V_2Te_2O_7F_2$

Crystal data

$V_2Te_2O_7F_2$
M_r = 507.38
Triclinic, $P\overline{1}$
a = 4.882 (2) Å
b = 5.112 (2) Å
c = 7.243 (3) Å
α = 108.17 (3)°
β = 91.64 (2)°
γ = 92.63 (2)°
V = 171.39 (12) Å^3
Z = 1
Mo $K\alpha$ radiation
μ = 11.12 mm^{-1}
T = 293 (2) K
0.05 × 0.03 × 0.02 mm

Data collection

Bruker–Nonius KappaCCD area-detector diffractometer
Absorption correction: multi-scan (*SADABS*; Bruker 2001)
T_{min} = 0.572, T_{max} = 0.800
5662 measured reflections
995 independent reflections
930 reflections with $I > 2\sigma(I)$
R_{int} = 0.023

Refinement

$R[F^2 > 2\sigma(F^2)]$ = 0.014
$wR(F^2)$ = 0.029
S = 1.07
995 reflections
62 parameters
$\Delta\rho_{max}$ = 0.64 e Å^{-3}
$\Delta\rho_{min}$ = −0.57 e Å^{-3}

The integrated intensities were corrected for absorption effects using a multi-scan method (*SADABS*; Bruker 2001). Structure solution by direct methods in the *Pnma* and $P\overline{1}$ space groups for $TiTeO_3F_2$ and $V_2Te_2O_7F_2$, respectively, followed by refinement of atomic coordinates and anisotropic displacement parameters, was performed using the programs *SHELXS97* and *SHELXL97* (Sheldrick, 2008) successively. In $TiTeO_3F_2$, the mixed site O4/F1, attested by the bond-valence study, was refined, constraining all coordinates and displacement components to be the same for atoms O4 and F1. The occupancy of the mixed site was fixed at 0.5 for each anion.

A residual electron-density peak of 4.26 e Å^{-3} persists at 0.7 Å from Te1, but it has no chemical or structural significance and cannot correspond to an additional anion. Refining the structure in the corresponding noncentrosymmetric space group $Pna2_1$ decreases the size of this residual peak to 2.6 e Å^{-3} but leads to a pseudocentrosymmetric structure with high correlations between variables, making it difficult to determine unambiguously the true space group. Nonlinear optical measurements have been performed on a powder sample, but no second harmonic generation (SHG) frequency doubling was observed; any slight distortion from a centrosymmetric structure should cause a detectable signal (Kurtz & Perry, 1968). Therefore, we conclude that the residual density peak results from the small size and limited diffraction quality of the single crystal rather than from an incorrect choice of space group.

For both compounds, data collection: *COLLECT* (Nonius, 1998); cell refinement: *DIRAX*/*LSQ* (Duisenberg, 1992); data reduction: *EVALCCD* (Duisenberg *et al.*, 2003); program(s) used to solve structure: *SHELXS97* (Sheldrick, 2008); program(s) used to refine structure: *SHELXL97* (Sheldrick, 2008); molecular graphics: *DIAMOND* (Brandenburg, 1999); software used to prepare material for publication: *SHELXL97*.

Supplementary data for this paper are available from the IUCr electronic archives (Reference: SQ3173). Services for accessing these data are described at the back of the journal.

References

Aldous, D. W., Goff, R. J., Attfield, J. P. & Lightfoot, P. (2007). *Inorg. Chem.* **46**, 1277–1282.
Brandenburg, K. (1999). *DIAMOND*. Crystal Impact GbR, Bonn, Germany.
Brown, I. D. (1981). *Structure and Bonding in Crystals*, Vol. 2, edited by M. O'Keeffe & A. Navrotsky, pp. 1–30. New York: Academic Press.
Bruker (2001). *SADABS*. Bruker AXS Inc., Madison, Wisconsin, USA.
Castro, A., Enjalbert, R. R., Lloyd, D., Rasines, I. & Galy, J. (1990). *J. Solid State Chem.* **85**, 100–107.
Crosnier-Lopez, M. P., Duroy, H. & Fourquet, J. L. (1994). *Z. Anorg. Allg. Chem.* **620**, 309–312.
Crosnier-Lopez, M. P., Duroy, H., Fourquet, J. L. & Abrabri, M. (1994). *Eur. J. Solid State Inorg. Chem.* **31**, 957–965.
Duisenberg, A. J. M. (1992). *J. Appl. Cryst.* **25**, 92–96.
Duisenberg, A. J. M., Kroon-Batenburg, L. M. J. & Schreurs, A. M. M. (2003). *J. Appl. Cryst.* **36**, 220–229.
Höss, P., Starkulla, G. & Schleid, T. (2005). *Acta Cryst.* E**61**, i113–i115.

Hyde, B. G. & Andersson, S. (1989). *Inorganic Crystal Structures*, pp. 19–20. New York: Wiley.
Ider, A., Frit, B., Laval, J. P., Carré, J., Claudy, P. & Létoffé, J. M. (1995). *Thermochim. Acta*, **258**, 117–124.
Ijjaali, I., Flaschenriem, C. & Ibers, J. A. (2003). *J. Alloys Compd*, **354**, 115–119.
Jennene Boukharrata, N., Laval, J.-P. & Thomas, P. (2008). *Acta Cryst.* C**64**, i57–i61.
Kurtz, S. K. & Perry, T. T. (1968). *J. Appl. Phys.* **39**, 3798–3813.
Laval, J. P., Jennene Boukharrata, N. & Thomas, P. (2008). *Acta Cryst.* C**64**, i12–i14.
Meier, S. F. & Schleid, Th. (2004). *Z. Naturforsch. Teil B*, **59**, 881–888.
Nonius (1998). *COLLECT*. Nonius BV, Delft, The Netherlands.
Sheldrick, G. M. (2008). *Acta Cryst.* A**64**, 112–122.
Shen, Y. L. & Mao, J. G. (2004). *J. Alloys Compd*, **385**, 86–89.
Weber, F. A., Meier, S. F. & Schleid, Th. (2001). *Z. Anorg. Allg. Chem.* **627**, 2225–2231.